A Journal of the Gesellschaft Deutscher Chemiker

Angewandte

GDCh

International Edition

Chemie

www.angewandte.org

Accepted Article

Title: Cationic Nitrogen Doped Helical Nanographenes

Authors: Kun Xu, Xinliang Feng, Reinhard berger, Alexey A Popov, Jan J Weigand, Ilka Vincon, Peter Machata, Felix Hennersdorf, Youjia Zhou, and Yubin Fu

To be cited as: *Angew. Chem. Int. Ed.* 10.1002/anie.201707714
Angew. Chem. 10.1002/ange.201707714

Link to VoR: http://dx.doi.org/10.1002/anie.201707714
http://dx.doi.org/10.1002/ange.201707714

WILEY-VCH

10.1002/anie.201707714

Charged Nanographene

DOI: 10.1002/anie.200((will be filled in by the editorial staff))

Cationic Nitrogen Doped Helical Nanographenes**

*Kun Xu, Yubin Fu, Youjia Zhou, Felix Hennersdorf, Peter Machata, Ilka Vincon, Jan J. Weigand, Alexey A. Popov, Reinhard Berger and Xinliang Feng**

Dedicated to Professor Klaus Müllen on the occasion of his 70th birthday

Abstract: *Herein, we report on the design and synthesis of a series of novel cationic nitrogen doped nanographenes (**CNDN**) with non-planar, axial chiral geometries. Single-crystal X-ray analysis reveals helical and cove-edged structures. Compared to their all-carbon analogues, the **CNDN** exhibit energetically lower lying frontier orbitals with a reduced optical energy gap and an electron accepting behavior. All derivatives show quasi reversible reductions in cyclic voltammetry. Depending on the number of nitrogen dopant, in situ spectroelectrochemistry proves the formation of neutral radicals (one nitrogen dopant) or radical cations (two nitrogen dopants) upon reduction. The concept of cationic nitrogen doping and introducing helicity into nanographenes pave the way for the design and synthesis of expanded nanographenes or even graphene nanoribbons containing cationic nitrogen doping.*

Nitrogen doped graphenes are fascinating materials due to their potential catalytic, optical and electronic applications[1] such as fuel cells,[1b] solar cells,[1c] sensors[1d] and transistors.[1e] Various top-down methods toward the synthesis of nitrogen doped graphene have been developed in the last decade.[1a] In particular, diverse types of nitrogen dopant have been found and classified as pyridinic, pyrrolic and graphitic ones, among which graphitic nitrogen is considered as one of the most active sites for the electrocatalysis.[2] From a molecular point of view, the graphitic-type nitrogen results from the replacement of a quaternary carbon atom with a nitrogen atom. This species leads to cationic nitrogen dopant, which changes the local density of states around the Fermi level and plays an important role in tailoring the electronic structure of the sp^2 carbon-frameworks.[2] However, controlling the nitrogen doping at specific positions of carbon materials at the molecular level (and with precise content) is a longstanding synthetic challenge.[1a,3]

Bottom-up organic synthesis offers the possibility to access nitrogen doped nanographenes with tailor-made structures and physical properties.[4,5] Although substantial efforts have been made in the synthesis of pyridinic[4d-j] and pyrrolic[4k-m] nitrogen containing nanographenes, cationic nitrogen doped nanographenes (**CNDN**) remain less available, mainly due to the synthetic difficulties. Pioneering work in the synthesis of **CNDN** has been carried out with planar structures (Figure 1, left),[5a-f] which revealed interesting optoelectronic properties as well as supramolecular behavior in solution, at the liquid-solid interface and in solid state.[5a-d] As our continuous efforts, we envisioned that the incorporation of helicity into the **CNDN** would provide unique graphene nanostructures with interfered π-electron delocalization and π-π interactions, which in turn influence their physical properties.[6-8] In addition, helicity provides nanographenes with chiral center, which renders the helical nanographenes as potential chiral material for applications such as organic spin filter.[9] To realize our hypothesis, herein we designed and synthesized a class of **CNDN** featured with helical[7] and cove-edge[8] structures exemplified for mono charged aza[5]helicene and doubly charged aza[4]helicenes in Figure 1.[10] The obtained charged nanographenes have energetically low lying frontier molecular orbitals with a pronounced stabilization of the lowest unoccupied molecular orbital (LUMO) causing a higher electron affinity and a reduced optical energy gap than their all-carbon analogies. Moreover, electrochemical and spectroelectrochemistry studies prove *in situ* formation of nitrogen containing neutral and cationic radicals depending on the number of nitrogen atoms. For the cationic double aza[4]helicenes, viologen-like properties and stable redox properties are revealed.

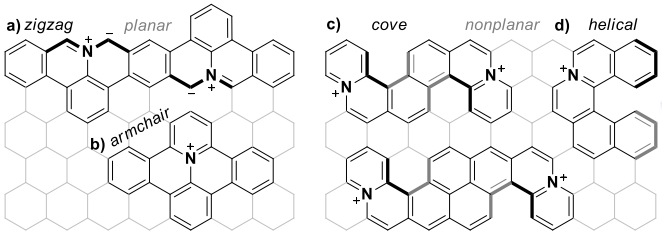

Figure 1. Cationic nitrogen doped graphene segments. a) planar zigzag edged nanaographene, b) planar armchair nanaographene, c) nonplanar cove edged nanographene (doubly charged aza[4]helicenes), d) nonplanar helical nanographene (mono charged aza[5]helicene)

We commenced our study with the synthesis of a series of singly charged nitrogen doped helical nanographenes. Via a rhodium catalyzed annulation process,[11] the desired charged aza[5]helicene trifluoracetate salt **1a** was obtained with 43% isolated yield (Scheme 1). Although in the literature reported procedure, oxygen was used as the oxidant for annulation reaction and excellent yields were obtained, in our case, the reaction was very sluggish and thus we optimized the conditions by using excess of silver trifluoroacetate. To avoid the possible aggregation of the helical structure in solution, an alkyne with bulky *tert*-butyl group, 1,2-bis(4-(*tert*-butyl)phenyl)ethyne was used as the annulation partner. With this conditions, we then extended to higher helical systems and larger conjugation. The annulation precursors (**2a-e**) were synthesized via Suzuki coupling according to

[*] Dr. K. Xu, Y. Fu, Y. Zhou, Dr. R. Berger, Prof. Dr. X. Feng
Center for Advancing Electronics Dresden (cfaed) & Department of Chemistry and Food Chemistry, Technische Universität Dresden
01062 Dresden (Germany)
E-mail: xinliang.feng@tu-dresden.de

F. Hennersdorf, Prof. Dr. J. J. Weigand
Chair of Inorganic Molecular Chemistry, Technische Universität Dresden, 01062 Dresden (Germany)

Dr. P. Machata, I. Vincon, Dr. A. A. Popov
Leibniz-Institute for Solid State and Materials Research, 01069 Dresden (Germany)

Supporting information for this article is available on the WWW under http://www.angewandte.org or from the author.

10.1002/anie.201707714

literature reported procedures (Supporting Information). To our delight, under similar reaction conditions, the corresponding racemic charged aza-[6] and [7] helicenes[12] (**1b**$^+$-**c**$^+$) were achieved in moderate yields (46% to 70%) after purification as their trifluoracetate salts (**1b**-**1c**). Charged aza-[5] and [6] helicenes with incorporated pyrene moiety (**1d**$^+$ and **1e**$^+$) afforded slightly better yields than those of **1a**$^+$ and **1b**$^+$ (Scheme 1). Considering the intrinsic challenge for the formation of the five-membered cyclometalated species with sterically hindered aromatic helical backbones[13] during the rhodium catalyzed C-H activation step according to the mechanism proposed by Huang and coworkers,[11] the yields of charged aza-[6] and [7] helicenes (**1b**$^+$-**c**$^+$ and **1e**$^+$) are remarkable. To the best of our knowledge, the charged aza[7]helicene **1c**$^+$ is the highest helicene with fully conjugated six-membered rings and cationic nitrogen doping.[13d-e]

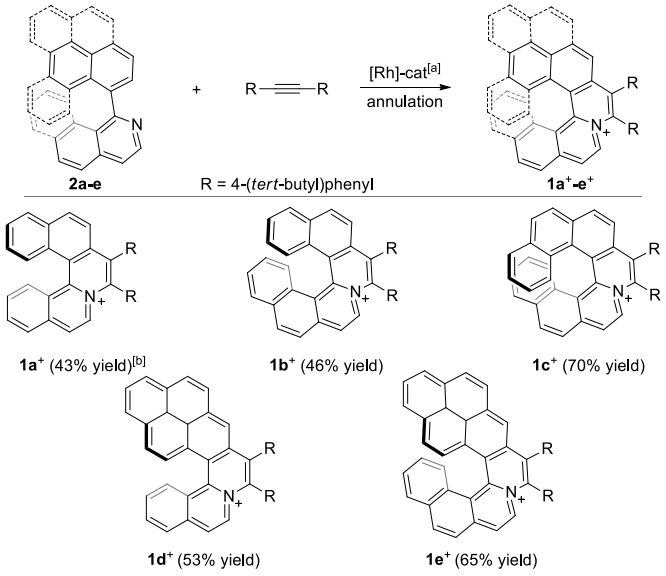

Scheme 1. Synthesis of cationic nitrogen doped helicenes **1a**$^+$-**e**$^+$. (a) Isoquinoline derivative **2a-e** (1.0 equiv), 1,2-bis(4-(*tert*-butyl)phenyl)ethyne (1.0 equiv), $[Cp^*RhCl_2]_2$ (20 mol%), AgO_2CCF_3 (2.0 equiv), MeOH (0.05 M), 120 °C, 20 hours. (b) The helicenes are obtained as trifluoroacetate salts (**1a**-**e**) in their racemic form.

Having had the success for the synthesis of monocharged nitrogen doped monohelicenes (**1a**$^+$-**e**$^+$), we then sought to the synthesis of larger **CNDN** with cove edge structures (namely, two cationic double aza[4]helicenes, **3a**$^{2+}$-**c**$^{2+}$). The corresponding precursors (**4a**-**4c**) were synthesized in one step via Suzuki coupling of 2-bromopyridine and easily available pinacol esters (**5a-c**). To our delight, compounds **3a**$^{2+}$-**c**$^{2+}$ were obtained in good to excellent yields in both Suzuki coupling (**4a-c**, 83-96%) and annulation (**3a**$^{2+}$-**c**$^{2+}$, 87-95%) steps (Supporting Information). To showcase the variability of the counter anion, for the synthesis of **3a**$^{2+}$-**c**$^{2+}$, silver triflate was employed to introduce triflate as the counter anion (**3a-c**).[14a]

Single crystals of monohelicenes **1b**$^+$, **1d**$^+$ and **1e**$^+$, as well as doubly charged aza-[4]helicenes **3a**$^{2+}$-**c**$^{2+}$, were successfully grown via slow evaporation of their dichloromethane/hexane solutions.[14b] As revealed in the crystal structures of **1b**$^+$, **1d**$^+$ and **1e**$^+$, the corresponding (*P*) and (*M*) isomers were observed, their interplanar angles are 41.28°, 44.59° and 45.48°, respectively (Figure 2, a). Remarkably enough, the interplanar angle of charged aza[6]helicene **1b**$^+$ (41.28°) is much smaller than the all-carbon [6]helicene (59.57°),[15] indicating a relatively less twisted configuration, possibly due to an attractive force stemmed from the unequal charge distribution (see Supporting Information for electrostatic potential map). The packing diagrams of **1b**$^+$, **1d**$^+$ and **1e**$^+$ show that the (*P*) and (*M*) isomers are arranged in an alternating fashion, while counter anions are distributed around the charged nitrogen center. More detailed crystal data were described in Supporting Information (S6).

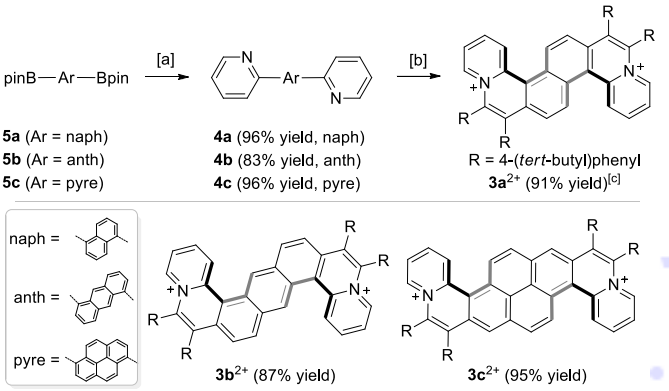

Scheme 2. Synthesis of cationic nitrogen doped cove edged nanographenes **3a**$^{2+}$-**c**$^{2+}$. (a) 2-bromopyridine (3.0 equiv), $Pd(PPh_3)_4$ (6 mol%), Na_2CO_3 (3.0 equiv), toluene/MeOH/H_2O (2/1/1), 90 °C, 15 hours. (b) 1,2-bis(4-(*tert*-butyl)phenyl)ethyne (2.0 equiv), $[Cp^*RhCl_2]_2$ (20 mol%), AgOTf (4.0 equiv), MeOH (0.05 M), 120 °C, 24 hours. (c) **3a**$^{2+}$-**c**$^{2+}$ are obtained as triflate salts (**3a**-**c**). Naph = naphthalene-1,5-diyl, anth = anthracene-1,5-diyl, pyre = pyrene-1,6-diyl.

Compound **3a**$^{2+}$ clearly show the nonplanar configuration (Figure 2b); chloride was observed as the counter anion, which might result from the purification or crystal growth process using chlorinated solvents. In the solid state, only (*M*,*M*) and (*P*,*P*) of **3a**$^{2+}$ were observed (Figure 2b), which suggested the higher stability of the concave type configuration than the (*M*,*P*)-isomer. The interplanar angles between the two terminal rings for cove edges are 38.50° and 39.26°, which are significantly larger than the reported [4]carbohelicene (24.87°).[16] The dihedral angles for both coves C4-C5-C6-C7 (17.71°) with C5-C6-C7-C8 (28.21°), and C16-C17-C18-C19 (17.84°) with C17-C18-C19-C20 (29.27°) are slightly different. The central naphthalene rings are distorted with torsion angles of 17.16° (C6-C7-C19-C20), 17.37° (C22-C6-C7-C19), 17.25° (C8-C7-C19-C18), and 19.30° (C7-C19-C18-C10). The high degree of distortion of the molecule results in the concave structure of **3a**$^{2+}$ with width of 11.179 Å, and depth of 1.615 Å (Figure 2b). Such type of concave structure may allow **3a**$^{2+}$ to be a potential 'bucky catcher' for fullerenes such as C60.[17] Compared to **3a**$^{2+}$, compound **3b**$^{2+}$ has interplanar angles of 17.66° and 17.74°, with width of 12.683Å and depth of 1.126Å for the concave core, which indicates a less distorted structure due to the extended π-spacer of the anthracene moiety. Notably, unlike **3a**$^{2+}$ and **3b**$^{2+}$, compound **3c**$^{2+}$ was only observed in its (*P*,*M*)/(*M*,*P*) form in the solid state, which may be due to the more rigid pyrene spacer.

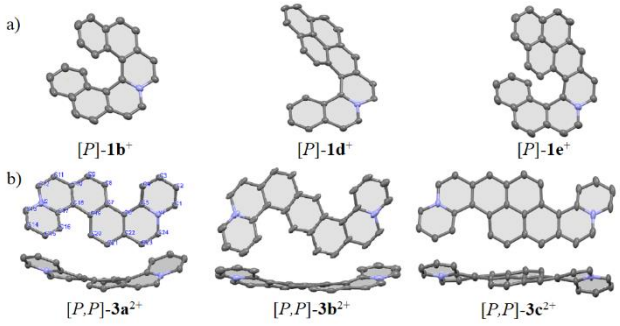

10.1002/anie.201707714

Figure 2. a) Molecular structure of [*P*]-**1b**$^{+}$ (left), [*P*]-**1d**$^{+}$ (middle), [*P*]-**1e**$^{+}$ (right) (4-(*tert*-butyl)phenyl, H and anions are omitted for clarity). b) Molecular structure of [*P,P*]-**3a**$^{2+}$ (left), [*P,P*]-**3b**$^{2+}$ (middle), [*P,M*]-**3c**$^{2+}$ (right) (top view and side view). Displacement ellipsoids are drawn at the 50% probability level.

To get further insight into the conformation of **3a**$^{2+}$ with doubly charged aza[4]helicene structure, DFT calculations at the B3LYP/6-31G+(d) level were performed by comparing the energy level of (*P*,*P*), (*M*,*M*) and (*M*,*P*) conformations (Figure 3). The optimized energy of meso-(*M*,*P*) is 2.4 kcal/mol higher than that of the (*P*,*P*) and (*M*,*M*) isomers. The isomerization from [*P*,*P*]-**3a**$^{2+}$ or [*M*,*M*]-**3a**$^{2+}$ to [*M*,*P*]-**3a**$^{2+}$ proceeds via the transition state [TS]-**3a**$^{2+}$ which has energy barrier of +8.6 kcal/mol. The higher thermodynamic stability of (*P*,*P*) or (*M*,*M*) isomers can explain why the (*M*,*P*) isomer was not identified in the crystal structures. Interestingly, the pristine (**3a'** without nitrogen doping) and the corresponding carbohelicene (**3a''** without substituents and nitrogen doping) of **3a**$^{2+}$ also favor their (*P*,*P*) and (*M*,*M*) isomers based on the calculated results. On the other hand, the isomerization energy of [*P*]-**1b**$^{+}$ to [*M*]-**1b**$^{+}$ is 35.5 kcal/mol, similar to the pristine **1b**$^{'}$ (36.4 kcal/mol, **1b**$^{+}$ without substituents) and full carbon hexahelicene **1b''** (37.2 kcal/mol). A detailed discussion can be found in S7 in the Supporting Information.

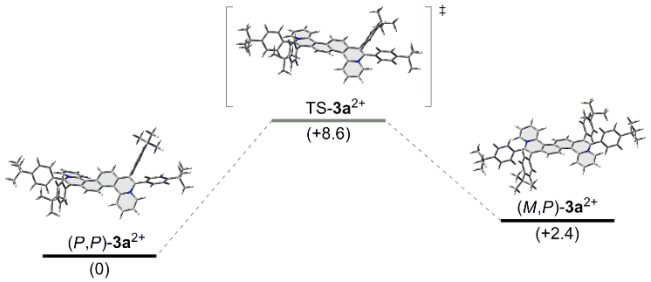

Figure 3. Isomerization process of **3a**$^{2+}$ from (*P*,*P*)-isomer to (*M*,*P*)-isomer. The relative Gibbs free energy (kcal/mol) was calculated at the B3LYP/6-31G+(d) level.

The photophysical properties of **1a**$^{+}$-**e**$^{+}$ and **3a**$^{2+}$-**c**$^{2+}$ were studied in CH_3CN solutions by UV-vis and photoluminescence spectroscopy (Figure 4). The absorption spectra of **3a**$^{2+}$, **3b**$^{2+}$ and **3c**$^{2+}$ exhibited maximum absorption peak at 335, 360 and 373 nm, respectively. This result suggests significant red-shift as the π-conjugation extends. The same trend was also observed for the helicenes **1a**$^{+}$-**1e**$^{+}$ ranging from 439 nm (**1a**$^{+}$) to 498 nm (**1e**$^{+}$). Based on the absorption onsets, the optical energy gaps for **3a**$^{2+}$, **3b**$^{2+}$ and **3c**$^{2+}$ are estimated to be 2.81, 2.69 and 2.33 eV, respectively. According to TD-DFT calculations (**3a**$^{2+}$-**c**$^{2+}$) (Supporting Information), the low-energy absorption bands from 400-550 nm are assignable to the HOMO→LUMO transitions. For cationic nitrogen doped monohelicenes, the optical energy gaps are from 2.68 eV (**1a**$^{+}$) to 2.20 eV (**1e**$^{+}$), suggesting that a relatively lower energy gap could be obtained by extending the conjugation system. All of the obtained compounds showed fluorescence in CH_3CN solution, with maximum emission peak ranging from 447 (**3a**$^{2+}$) to 600 nm (**1e**$^{+}$). In comparison with literature reported maximum absorptions for [5], [6] and [7]carbohelicenes (395, 413 and 425 nm, respectively),[18] the maximum absorptions of cationic nitrogen doped [5], [6] and [7]helicenes (439, 448 and 469 nm for **1a**$^{+}$, **1b**$^{+}$ and **1c**$^{+}$, respectively) show bathochromic shift of 35 to 44 nm, implying that the cationic nitrogen doping could lower the optical energy gap of the helicene system.

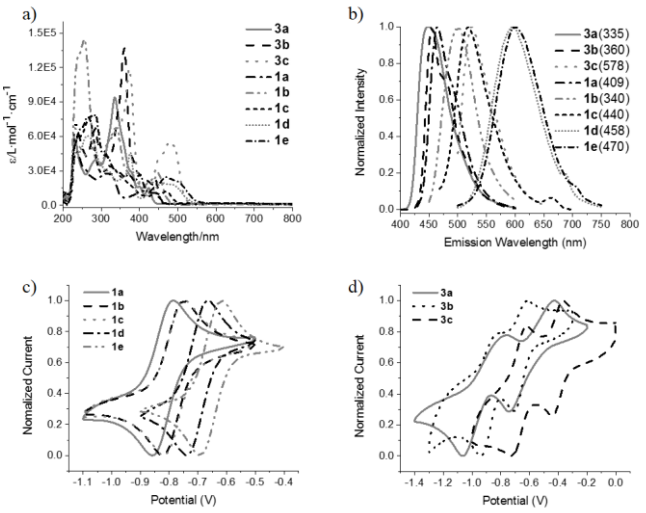

Figure 4. a) UV/Vis spectra in 1.0 x 10^{-5} M CH_3CN (top left). b) Fluorescence spectra in 1.0x10^{-7} M CH_3CN (top right, excitation wavelengths are given in parenthesis). c) Cyclic voltammetry in a solution of Bu_4NPF_6 (0.1 M) in DCM at room temperature, using Ag wire as reference electrode and ferrocene/ferrocenium (Fc/Fc^{+}) as external standard, with scan rate of 0.05 V/s for **1a**-**e** (CF_3CO_2 salts of **1a**$^{+}$-**e**$^{+}$, bottom left), 1.0 V/s for **3a**-**c** (OTf salts of **3a**$^{2+}$-**c**$^{2+}$ bottom right).

The electrochemical behavior of **CNDN** were investigated by cyclic voltammetry in dichloromethane solution. The reduction of charged azahelicenes **1a**$^{+}$-**e**$^{+}$ provided one quasi reversible peak in a potential range of -0.86 V to -0.69 V vs Ag/Ag^{+}. Notably, compounds **3a**$^{2+}$-**c**$^{2+}$ exhibited two quasi reversible reduction peaks, indicating the formation of radical cations (first reduction) and neutral species (second reduction). This result suggests their potential to be used as viologen type materials.[19] Using ferrocene as an external standard, energy levels of the LUMO of monohelicenes are determined to be -3.25 (**1a**$^{+}$), -3.29 (**1b**$^{+}$) and -3.42 eV (**1c**$^{+}$). For the cove edge nitrogen doped nanographenes, energy levels of the LUMO are derived to be -3.59 (**3a**$^{2+}$), -3.41 (**3b**$^{2+}$) and -3.60 eV (**3c**$^{2+}$). Based on the LUMO and optical energy gap values, the corresponding HOMOs -6.30 (**3a**$^{2+}$), -6.10 (**3b**$^{2+}$) and -6.00 eV (**3c**$^{2+}$) are derived respectively. All optoelectronic data of **1a**$^{+}$-**e**$^{+}$ and **3a**$^{2+}$-**c**$^{2+}$ as well as a comparison with their pristine carbon analogues are provided in Table 7 in the Supporting Information.

To evaluate the role of cationic nitrogen doping, DFT calculations of **1b**$^{+}$ and **3a**$^{2+}$, their pristine structures (**1b'** and **3a'**) as well as their all carbon analogies (**1b''** and **3a''**) were performed (Supporting Information, Table 7). The calculated LUMO values (E^{th}_{LUMO}) are in good agreement with experimental LUMOs (E_{LUMO}), while calculated HOMOs (E^{th}_{HOMO}) differ the HOMOs (E_{HOMO}) derived from optical energy gap (E_g) and E_{LOMO} in the range of 0.63-0.94 eV due to polarization effects. In comparison with their all-carbon analogies, their HOMO values are lowered by 0.8 eV (**1b**$^{+}$ *vs* **1b''**) and 1.16 eV (**3a**$^{2+}$ *vs* **3a''**), and LUMO values are lowered by 1.4 eV (**1b**$^{+}$ *vs* **1b''**) and 1.87 eV (**3a**$^{2+}$ *vs* **3a''**). The strong effect on the LUMO levels renders them with electron accepting properties. Noteworthy, substituents (*4*-(*tert*-butyl)phenyl) could also lower the HOMO and LUMO values (**1b**$^{+}$ *vs* **1b'** and **3a**$^{2+}$ *vs* **3a'**), which offers the possibility to finely tune the electronic nature via modifying the substituents of **CNDN**.

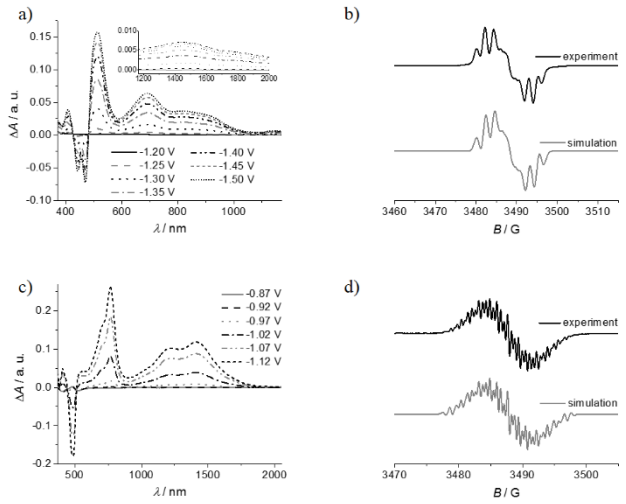

Figure 5. a) UV/vis/NIR spectra measured during electrochemical reduction of **1c**$^{+}$ (top left). b) Experimental and simulated EPR spectra of the reduced form of **1c**$^{+}$ (top right). c) UV/vis/NIR spectra measured during the first redox step (radical cation) of **3c**$^{2+}$ (bottom left). d) Experimental and simulated EPR spectra of the radical cation form of **3c**$^{2+}$ (bottom right).

Inspired by these cyclic voltammetry and DFT calculation results, detailed spectroscopic characterizations by *in situ* EPR (electron paramagnetic resonance) and UV/vis/NIR absorption spectroscopy were performed for compounds **1c**$^{+}$ and **3c**$^{2+}$ as representative examples. Figure 5 shows the spectra measured during cyclic voltammetry of **1c**$^{+}$ at its reduction step. The formation of the neutral radical [**1c**]$^{\bullet}$ is accompanied by depletion of the absorption of **1c**$^{+}$ at 469 nm and appearance and growth of new absorption bands at 513, 692, and 817 nm (the latter is broad and extended to ca 1000 nm). Weak absorption is also found at 1450 nm (Figure 4a). EPR measurements (performed simultaneously with optical spectroscopy) confirm the formation of the stable helical radical.[20] The spin density in the radical is distributed over the azahelicene backbone and does not extend to the substituents (4-(*tert*-butyl)phenyl). The hyperfine structure of the experimental EPR spectrum is reproduced well with the coupling constants of four protons and the nitrogen, all near or exceeding 2 G (Figure 6 and Supporting Information). Even more, the *in situ* generated radical cation [**3c**]$^{\bullet+}$ upon one electron reduction (first reduction of **3c**$^{2+}$) was clearly proved by *in situ* electrochemistry studies. As depicted in Figure 5c, the radical cation shows intense absorption bands peaked at 766, 1200 and 1410 nm. EPR spectrum (Figure 5d) further proved the presence of radical cation [**3c**]$^{\bullet+}$. The two electron reduced neutral species [**3c**]$^{\cdot\cdot}$ (second reduction of **3c**$^{2+}$), although highly unstable, was also observed via *in situ* UV/vis/NIR (Supporting Information).

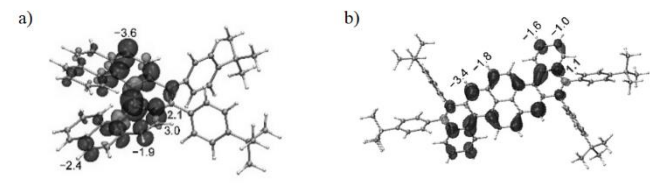

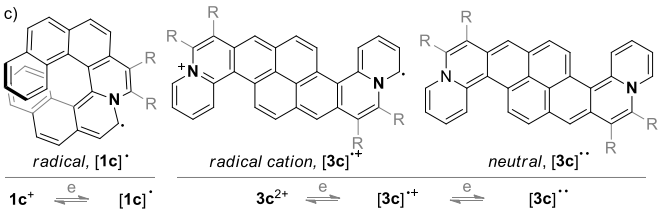

Figure 6. a) DFT-computed spin density distribution and main hyperfine coupling constants (in Gauss; black – protons, blue - nitrogen) in the radical form of **1c**$^{+}$ ([**1c**]$^{\bullet}$, top left). b) DFT-computed spin density distribution and main hyperfine coupling constants (in Gauss; black – protons, blue - nitrogen) in the radical cation form of **3c**$^{2+}$ ([**3c**]$^{\bullet+}$, top right). c) Chemical structures of *in situ* generated neutral radical [**1c**]$^{\bullet}$, radical cation [**3c**]$^{\bullet+}$ upon first reduction of **3c**$^{2+}$ and neutral species [**3c**]$^{\cdot\cdot}$ upon second reduction of **3c**$^{2+}$. R = 4-(*tert*-butyl)phenyl.

To conclude, we have designed and synthesized a novel class of **CNDN** with cove edges and helical structures. These molecules exhibit unique nonplanar configurations with axial chirality. The lower lying HOMOs/LUMOs and energy gaps, as well as quasi reversible electrochemical reduction allow the *in situ* characterization of their reduced radical and cationic radical species. These results imply their potential as (opto)electronic materials. The concept of cationic nitrogen doping and introducing helicity into nanographenes holds promise for our ongoing design and synthesis of **CNDN** with expanded π-systems, multiple doping centers, novel nonplanar structures and even graphene nanoribbons.

Acknowledgements

This research was supported financially by ERC grants on 2DMATER, the EC under Graphene Flagship (No. CNECT-ICT-604391), the Center for Advancing Electronics Dresden (cfaed), the European Social Fund, and the Federal State of Saxony (ESF-Project "GRAPHD", TU Dresden). We thank Ji Ma, Shunqi Xu, Dr. Ajayakumar Murugan Rathamony, Dr. Junzhi Liu, Dr. Jian Zhang, Dr. Stavroula Sfaelou and Dr. Xiaodong Zhuang for helpful discussions. JJW thanks the DFG for funding a diffractometer (INST269/618-1).

Conflict of interest

The authors declare no conflict of interest.

Keywords: Nanographene · Nitrogen doping · Polycyclic aromatic hydrocarbon · Helicene · Graphene

[1] a) Review on Recent Progress in Nitrogen-Doped Graphene: H. Wang, T. Maiyalagan, X. Wang, *ACS Catal*. **2012**, *2*, 781-794. b) D. Guo, R. Shibuya, C. Akiba, S. Saji, T. Kondo, J. Nakamura, *Science* **2016**, *351*, 361-365. c) Y. Xue, J. Liu, H. Chen, R. Wang, D. Li, J. Qu, L. Dai, *Angew. Chem. Int. Ed*. **2012**, *51*, 12124-12127; *Angew. Chem*. **2012**, *124*, 12290-12293. d) Y. Wang, Y. Shao, D. W. Matson, J. Li, Y. Lin, *ACS Nano*. **2010**, *4*, 1790-1798. e) O. S. Kwon, S. J. Park, J. Hong, A. Han, J. S. Lee, J. S. Lee, J. H. Oh, J. Jang, *ACS Nano*. **2012**, *6*, 1486-1493.

[2] a) W. J. Lee, U. N. Maiti, J. M. Lee, J. Lim, T. H. Han, S. O. Kim, *Chem. Commun*. **2014**, *50*, 6818-6830. b) J. Kim, K. Lee, S. I. Woo, Y. Jung, *Phys. Chem. Chem. Phys*. **2011**, *13*, 17505-17510.

[3] D. Wei, Y. Liu, *Adv. Mater*. **2010**, *22*, 3225-3241.

[4] Examples of bottom-up synthesis of nitrogen doped nanographenes and graphene nanoribbons: a) K. T. Kim, J. W. Lee, W. H. Jo, *Macromol.*

Chem. Phys. **2013**, *214*, 2768-2773. b) T. H. Vo, M. Shekhirev, D. A. Kunkel, F. Organe, M. J. F. Guinel, A. Enders, A. Sinitskii, *Chem. Commun*. **2014**, *50*, 4172-4174. c) D. J. dibble, Y. S. Park, A. Mazaheripour, M. J. Umerani, J. W. Ziller, A. A. Gorodetsky, *Angew. Chem. Int. Ed*. **2015**, *54*, 5883-5887; *Angew. Chem.* **2015**, *127*, 5981-5985. d) Y. S. Park, D. J. Dibble, J. Kim, R. C. Lopez, E. Vargas, A. A. Gorodetsky, *Angew. Chem. Int. Ed*. **2016**, *55*, 3352-3355; *Angew. Chem.* **2016**, *128*, 3413-3416. e) U. H. F. Bunz, *Acc. Chem. Res*. **2015**, *48*, 1676-1686. f) S. M. Draper, D. J. Gregg, R. Madathil, *J. Am. Chem. Soc*. **2002**, *124*, 3486-3487. g) S. M. Draper, D. J. Gregg, E. R. Schofield, W. R. Browne, M. Dati, J. G. Vos, P. Passaniti, *J. Am. Chem. Soc*. **2004**, *126*, 8694-8701. h) L. P. Wijesinghe, B. S. Lankage, G. M. Ó Máille, S. D. Perera, D. Nolan, L. Wang, S. M. Draper, *Chem. Commun*. **2004**, *50*, 10637-10640. i) J. Wei, B. Han, Q. Guo, X. Shi, W. Wang, N. Wei, *Angew. Chem. Int. Ed*. **2010**, *49*, 8209-8213; *Angew. Chem.* **2010**, *122*, 8385-8389. j) B. He, A. B. Pun, L. M. Klivansky, A. M. McGough, Y. Ye, J. Zhu, J. Guo, S. J. Teat, Y. Liu, *Chem. Mater*. **2014**, *26*, 3920-3927. k) M. Takase, V. Enkelmann, D. Sebastiani, M. Baumgarten, K. Müllen, *Angew. Chem. Int. Ed*. **2007**, *46*, 5524-5527; *Angew. Chem.* **2007**, *119*, 5620-5623. l) M. Takase, T. Narita, W. Fujita, M. S. Asano, T. Nishinaga, H. Benten, K. Yoza, K. Müllen, *J. Am. Chem. Soc*. **2013**, *135*, 8031-8040. m) E. Gońka, P. J. Chmielewski, T. Lis, M. Stępień, *J. Am. Chem. Soc*. **2014**, *136*, 16399-16410.

[5] a) D. Wu, L. Zhi, G. J. Bodwell, G. Cui, N. Tsao, K. Müllen, *Angew. Chem. Int. Ed.* **2007**, *46*, 5417-5420; *Angew. Chem.* **2007**, *119*, 5513-5516. b) D. Wu, W. Pisula, V. Enkelmann, X. Feng, K. Müllen, *J. Am. Chem. Soc*. **2009**, *131*, 9620-9621. c) D. Wu, R. Liu, W. Pisula, X. Feng, K. Müllen, *Angew. Chem. Int. Ed.* **2011**, *50*, 2791-2794; *Angew. Chem.* **2011**, *123*, 2843-2846. d) K. S. Malli, D. Wu, X. Feng, K. Müllen, M. V. der Auweraer, S. D. Feyter, *J. Am. Chem. Soc.* **2011**, *133*, 5686-5688. e) R. Berger, A. Giannakopoulos, P. Ravat, M. Wagner, D. Beljonne, X. Feng, K. Müllen, *Angew. Chem. Int. Ed.* **2014**, *53*, 10520-10524; *Angew. Chem.* **2014**, *126*, 10688-10692. f) R. Berger, M. Wagner, X. Feng, K. Müllen, *Chem. Sci*. **2015**, *6*, 436-441. S. Ito, Y. Tokimaru, K. Nozaki, *Chem. Commun*, **2015**, *51*, 221-224.

[6] a) E. Clar, J. F. Stephen, *Tetrahedron* **1965**, *21*, 467-470. b) S. Xiao, M. Myers, Q. Miao, S. Sanaur, K. Pang, M. L. Steigerwald, C. Nuckolls, *Angew. Chem. Int. Ed*. **2005**, 44, 7390-7394; *Angew. Chem.* **2005**, 117, 7556-7560. c) S. Xiao, S. J. Kang, Y. Wu, S. Ahn, J. B. Kim, Y. Loo, T. Siegrist, M. L. Steigerwald, H. Li, C. Nuckolls, *Chem. Sci*. **2013**, *4*, 2018-2023. d) J. Liu, B. Li, Y. Tan, A. Giannakopoulos, C. Sanchez-Sanchez,D. Beljonne, P. Ruffieux, R. Fasel, X. Feng, K. Müllen, *J. Am. Chem. Soc*. **2015**, *137*, 6097-6103. e) J. Ma, J. Liu, M. Baumgarten, Y. Fu, Y. Tan, K. S. Schellhammer, F. Ortmann, G. Cuniberti, H. Komber, R. Berger, K. Müllen, X. Feng, *Angew. Chem. Int. Ed*. **2017**, *56*, 3280-3284; *Angew. Chem.* **2017**, *129*, 3328-3332.

[7] M. Ball, Y. Zhong, Y. Wu, C. Schenck, F. Ng, Michael, Steigerwald, S. Xiao, C. Nuckolls, *Acc. Chem. Res.* **2015**, *48*, 267-276.

[8] a) Y. Shen, C. Chen, *Chem. Rev*. **2012**, *112*, 1463-1535. b) M. Gingras, *Chem. Soc. Rev*. **2013**, *42*, 968-1006. c) M. Gingras, G. Félix, R. Peresutti, *Chem. Soc. Rev*. **2013**, *42*, 1007-1050. d) M. Gingras, *Chem. Soc. Rev*. **2013**, *42*, 1051-1095.

[9] a) V. Kiran, S. P. Mathew, S. P. Cohen, I. H. Delgado, J. Lacour, R. Naaman, *Adv. Mater.* **2016**, *28*, 1957-1962. b) R. Naaman, D. H. Waldeck, *Annu. Rev. Phys. Chem.* **2015**, *66*, 263-281.

[10] The "cove-edge" in nanographenes is identified as a [4]helicene.

[11] G. Zhang, L. Yang, Y. Wang, Y. Xie, H. Huang, *J. Am. Chem. Soc.* **2013**, *135*, 8850-8853.

[12] a) S. Arai, T. Takeuchi, M. Ishikawa, T. Takeuchi, M. Yamazaki, M. Hida, *J. Chem. Soc. perkin Trans. I.* **1987**, 481-487. b) S. Arai, T. Yafune, M. Okubo, M. Hida, *Tetrahedron Lett*. **1989**, *30*, 7217-7218. c) S. Arai, M. Ishikura, K. Sato, T. Yamagishi, *J. Heterocyclic Chem*. **1995**, *32*, 1081-1083. d) K. Sato, Y. Katayama, T. Yamagishi, S. Arai, *J. Heterocyclic Chem*. **2006**, *43*, 177-181. e) L. Severa, M. Ončák, D. Koval, R. Pohl, D. Šaman, I. Císařová, P. E. Reyes-Gutiérrez, P. Sázelová, V. Kašička, F, Teplý, P. Slavíček, *Angew. Chem. Int. Ed*. **2012**, *51*, 11972-11976; *Angew. Chem.* **2012**, *124*, 12138-12141.

[13] J. Zheng, S. You, *Angew. Chem. Int. Ed*. **2014**, *53*, 13244-13247; *Angew. Chem.* **2014**, *126*, 13460-13463.

[14] a) Based on previous published results (see ref. 5a-c), we speculate the counter anions will have large influence on the packing structure of the cationic nitrogen doped nanographenes, detailed study will be presented in our future work. b) Compound **4a** and **4c**, were not possible to measure due to insufficient qualities of their crystals.

[15] a) M. S. Newman, D. Lednicer, *J. Am. Chem. Soc*. **1956**, *78*, 4765-4770. b) T. Hahn, *Acta Cryst*. **1958**, *11*, 825.

[16] F. H. Herbstein, G. M. J. Schmidt, *J. Chem. Soc*. **1954**, 3302-3313.

[17] E. M. Pérez, N. Martín, *Chem. Soc. Rev*. **2008**, *37*, 1512-1519.

[18] a) E. Clar, D. G. Stewart, *J. Am. Chem. Soc*. **1952**, *74*, 6235-6238. b) M. S. Newman, D. Lednicer, *J. Am. Chem. Soc*. **1956**, *78*, 4765-4770. b) M. Flammang-Barbieux, J. Nasielski, R. H. Martin, *Tetrahedron Lett.* **1967**, *8*, 743-744.

[19] a) S. Rochat, T. M. Swager, *Angew. Chem. Int. Ed*. **2014**, *53*, 9792-9796; *Angew. Chem.* **2014**, *126*, 9950-9954. b) D. Jiriya, M. Tosun, P. Zhao, J. S. Kang, A. Javey, *J. Am. Chem. Soc*. **2014**,136, 7853-7856. c) E. Hwang, S. Seo, S. Bak, H. Lee, M. Min, H. Lee, *Adv. Mater*. **2014**,26, 5129-5136.

[20] a) P. Ravat, T. Šolomek, M. Rickhaus, D. Häussinger, M. Neuburger, M. Baumgarten, M. Juríček, *Angew. Chem. Int. Ed*. **2016**, *55*, 1183-1186; *Angew. Chem.* **2016**, *128*, 1198-1202. b) P. Ravat, P. Ribar, M. Rickhaus, D. Häussinger, M. Neuburger, M. Juríček, *J. Org. Chem.* **2016**, 81, 12303-12317.

Received: ((will be filled in by the editorial staff))
Published online on ((will be filled in by the editorial staff))

10.1002/anie.201707714

Charged Nanographene

Kun Xu, Yubin Fu, Youjia Zhou, Felix Hennersdorf, Peter Machata, Ilka Vincon, Jan J. Weigand, Alexey A. Popov, Reinhard Berger and Xinliang Feng* _____ **Page – Page**

Cationic Nitrogen Doped Helical Nanographenes

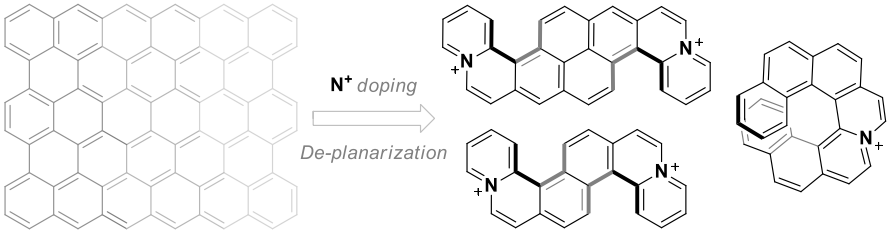

Nitrogen Plus: Engineering of nanographenes via a new bottom-up synthetic method towards cationic nitrogen doped nanographenes with nonplanar helical structures is described. The protocol provides easy access to novel types of cationic nitrogen doped nanographenes with interesting properties, which holds the potential as optical and electronic materials.